

NASA CR-72885

N71-28326

TOPICAL REPORT

SPACE CHARGE EFFECTS IN A
VACUUM THERMIONIC DIODE

by

Anthony J. Cassano

CONSOLIDATED CONTROLS CORPORATION
15 Durant Avenue
Bethel, Connecticut 06801

prepared for

NATIONAL AERONAUTICS AND SPACE ADMINISTRATION

April 30, 1971

CONTRACT NAS 3-4170

NASA Lewis Research Center
Cleveland, Ohio
James P. Couch, Project Manager
Space Power Systems Division

**CASE FILE
COPY**

TABLE OF CONTENTS

| <u>Title</u> | <u>Page No.</u> |
|---------------------------------------|-----------------|
| Abstract | iii |
| Summary | 1 |
| Introduction | 2 |
| Space Charge Model (Zero-Current) | 7 |
| Space Charge Model (non-Zero-Current) | 12 |
| Experimental Program | 15 |
| Summary of Results | 18 |

LIST OF ILLUSTRATIONS

| <u>Fig. No.</u> | <u>Title</u> | <u>Page No.</u> |
|---------------------|--|---------------------|
| 1 | Electron Potential Energy Diagram | 21 |
| 2 | Zero-Current Potential Energy Diagram, Low Collector Work Function | 22 |
| 3 | Zero-Current Potential Energy Diagram, High Collector Work Function | 23 |
| 4 | Applied Diode Voltage as Function of Collector Work Function | 24 |
| 5 | Zero-Current Potentials as Functions of Collector Temperature | 25 |
| 6 | Applied Diode Voltage as Function of Collector Temperature | 26 |
| 7 | Non-Zero-Current Potential Energy Diagram | 27 |
| 8 | Space Charge Curves, 1600°F Collector | 28 |
| 9 | Space Charge Curves, 1400°F Collector | 29 |
| 10 | Space Charge Curves, 1200°F Collector | 30 |
| 11 | Space Charge Curves, 1000°F Collector | 31 |
| 12 | Space Charge Curves, 1200°F Collector | 32 |
| 13 | Space Charge Curves, 1400°F Collector | 33 |
| 14 | Space Charge Curves, 1600°F Collector | 34 |
| 15 | Space Charge Curves, 1600°F Collector | 35 |
| 16 | Space Charge Curves, 1400°F Collector | 36 |
| 17 | Space Charge Curves, 1200°F Collector | 37 |
| 18 | Space Charge Curves, 1000°F Collector | 38 |
| 19 | Space Charge Curves, 1200°F Collector | 39 |
| 20 | Space Charge Curves, 1400°F Collector | 40 |
| 21 | Space Charge Curves, 1600°F Collector | 41 |

ABSTRACT

In the standard treatment of space-charge effects in a vacuum thermionic diode, it is customary to assume a negligible contribution from the collector electrode. However, as the collector temperature increases, its contribution to the diode voltage-current relationship must be considered. A refined diode space-charge model has been developed which includes emission from both the emitter and collector electrodes. The analysis was checked by vacuum diode experiments conducted over a collector temperature range of 1000-1600°F. Reasonable correlation was obtained, indicating the validity of the model.

SUMMARY

The determination of the space charge parameters of a vacuum thermionic diode is an effective check on diode performance. However, correlation between theory and experiment presents two problems. First, the standard space charge treatment assumes a negligible contribution from the collector electrode. Second, the theoretical diode driving voltage is an internal parameter, not readily available experimentally.

The aim of this effort was to resolve these two difficulties. A refined space charge model was developed which included collector contributions to the diode current, the effects of changes in the collector surface conditions, and the evaluation of the importance of collector temperature. Secondly, the model resulted in a set of master space charge curves for collector temperatures between 1000 and 2000°F. These master curves were prepared using diode current and diode applied voltage, a readily available experimental quantity, as parameters.

The model was checked against experiments conducted on operating diodes over a collector temperature range of 1000-1600°F and reasonable correlation was obtained.

At high diode current levels, the effect of changes in collector work function was quite apparent and resulted in deviations from the master curves. It may be concluded that meaningful evaluation of an operating diode at collector temperatures above 1000°F may be made by using the master curves but repeatable diode operation depends strongly on consistent collector work function characteristics.

INTRODUCTION

In a vacuum thermionic diode, an emitter electrode is heated and a positive voltage is applied to a collector electrode. Thermal energy due to the emitter temperature raises the energy level of the electrons to the point where they are capable of escaping the emitter surface. The emitter electrons move across the inter-electrode gap, from the emitter to the collector, with a finite increasing velocity. As the temperature of the emitter (and the associated electron emission) is increased, the number of electrons in the interelectrode space increases. This increase continues up to a point determined by the emitter-collector voltage. However, as the temperature is further increased, the repulsive force due to the interelectrode electrons balances the attractive force of the collector voltage at the emitter surface. Any further temperature increase results in the repulsive force becoming greater than the attractive force and the additional emitted electrons return to the emitter surface. The emitter-collector current therefore reaches a limit for a given collector voltage and will show very little further increase as emitter temperature exceeds this critical value.

The space charge effect denotes the repulsive force acting on the emitted electrons due to the electron cloud in the inter-electrode space. Figure 1 presents the usual potential energy diagrams related to these statements. The symbols used in Figure 1 are as follows.

- FL_C: Collector Fermi level energy
- FL_e: Emitter Fermi level energy
- V₂: Voltage applied to the diode
- V₃: Potential barrier referred to collector
- V₄: Emitter potential barrier
- V₅: Potential due to space charge effect
- V₆: Effective emitter-collector potential difference
- φ_C: Collector work function
- φ_e: Emitter work function
- D₁: Emitter-collector distance
- D₂: Emitter to maximum space charge distance.
- D₃: Collector to maximum space charge distance

Curves A, B, C, depict situations for increasing temperature at constant voltage. Curve A is for low temperature (emission limited). The potential gradient is constant from emitter to collector. When the temperature is raised to the critical value mentioned above, Curve B is obtained. For this condition the potential gradient is zero at the emitter surface. A further increase in temperature results in Curve C, where the space charge creates a virtual emitter at distance D₂ from the actual emitter surface. In distance D₂, there exist currents flowing in both directions between the emitter and the maximum space charge potential plane. In D₃, current flows only towards the collector. Therefore, V₆ becomes the effective diode potential difference. This assumes that there will be no electron reflection off the collector surface and that the collector-emitter electron current is negligible.

Thermal energy due to the emitter temperature raises electrons over the potential barrier V_4 composed of the emitter work function ϕ_e and the space charge potential V_5 . They are then attracted to the collector surface by potential V_6 . Any kinetic energy gained by the electrons is dissipated as heat when the electrons reach the collector. Upon entering the collector, the electrons lose potential ϕ_c and fall to the collector Fermi level from which point they are raised, by the applied voltage V_2 , to the emitter Fermi level. The cycle then repeats itself. The two basic equations describing the diode current are the Langmuir-Child relation for operation in the space charge limited mode (see Curve C of Figure 1)

$$I = 2.34 \times 10^{-6} \frac{(V_6)^{3/2} A}{(D_2)^2} \quad \text{amperes} \quad (1)$$

and the Richardson-Dushman relation for the emission capability of a surface (emission limited condition).

$$I_s = 120(T_1)^2 A \exp - \frac{(e\phi_e)}{K \cdot T_1} \quad \text{amperes} \quad (2)$$

where T_1 is the emitter temperature ($^{\circ}K$), e is the electronic charge (1.60×10^{-19} coulomb), K is the Boltzmann constant (1.38×10^{-23} joule/ $^{\circ}K$) and A is the emitting surface area. Equation 2 represents the diode current for emitter temperature up to the critical temperature resulting in Curve B of Figure 1. This point is an important diode condition separating the emission limited and space charge limited regions.

As the temperature is increased further, a space charge potential is developed and a virtual emitter is created at the position D2 from the emitter with an effective work function $V4 = (\phi_e + V5)$. This condition is represented by Curve C of Figure 1. Therefore, the Richardson-Dushman relation can be written for the space charge limited condition.

$$I = 120(T1)^2 A \exp - \frac{e(\phi_e + V5)}{K \cdot T1} \quad \text{amperes} \quad (3)$$

Equations 1 and 3 are both valid representations for the space charge limited current. Equation 1 indicates the distance and voltage dependence while Equation 3 is useful in treating the emitter work function and temperature parameters.

Standard treatments of these conditions usually assume that the collector-emitter electron current is negligible. In the majority of cases, the collector temperature is low enough to make this a reasonable assumption. However, for some high-temperature applications, the collector temperature and the possible development of low-work-function collector surfaces indicate that collector emission may not be ignorable. In addition, as diode current changes, the virtual-emitter location affects the spacing parameter in Child's space-charge equation.

Space-Charge conditions may be analyzed in two aspects; the zero-current condition (positive voltage applied to the emitter) and the non-zero-current condition (positive voltage applied to the collector). Using these two conditions, a refined space-charge model has been developed which includes emission from both electrodes, is independent of their work-functions, and

corrects for motion of the virtual emitter. Experimental results have been evaluated against this model and good agreement has been obtained.

SPACE CHARGE MODEL (ZERO-CURRENT)

The zero-current model is based on equal and opposite electron flow from the emitter and collector. For this condition to exist, it normally is necessary to apply a positive voltage to the emitter. This voltage enhances collector emission, since the collector temperature is not usually high enough to fully offset emitter electron-flow. When the collector work function is sufficiently low, the potential energy diagram is as shown in Figure 2, with I_1 and I_2 referring to emitter and collector current flow, respectively. The zero-potential-gradient plane, corresponding to the position of the virtual emitter, is located in the inter-electrode gap. Under these conditions, the model is determined completely by the mechanical spacing (D_1) of the diode and the emitter and collector temperatures (T_1 and T_2).

Nottingham (Reference 1) presents a universal relation between current, temperature and distance, subject to the condition $(V_4 - \phi_e) > V_5$; i.e. existence of space charge limitation. When applied to the emitter and collector currents, the relation yields the following.

$$I_1 = 7.729 \times 10^{-12} (T_1)^{3/2} \frac{A}{(D_2)^2} \text{ amperes} \quad (4)$$

$$I_2 = 7.729 \times 10^{-12} (T_2)^{3/2} \frac{A}{(D_3)^2} \text{ amperes} \quad (5)$$

Under zero-current conditions, $I_1 = I_2$ or

$$\frac{(T_1)^{3/2}}{(D_2)^2} = \frac{(T_2)^{3/2}}{(D_3)^2}$$

$$D_3 = \left(\frac{T_2}{T_1}\right)^{3/4} D_2 = M \cdot D_2 \quad (6)$$

Since $D_1 = D_2 + D_3,$

$$D_2 = \frac{D_1}{(1 + M)} \quad (7)$$

and $D_3 = \frac{M \cdot D_1}{(1 + M)} \quad (8)$

Equations 7 and 8 relate the distances D_2 and D_3 to the distance D_1 , the mechanical spacing of the diode, using the electrode temperatures expressed as the parameter $M = (T_2/T_1)^{3/4}$. In this way, the emitter and collector current contributions may be calculated from Equations 4 and 5.

It is desirable from an experimental standpoint to be able to relate the zero-current condition to the applied voltage V_2 , a directly measurable parameter.

Since the electrode currents are unique functions of temperature and distance (Equations 4 and 5), corresponding unique relations may be obtained for the potential barrier parameters V_3 and V_4 . (Reference 1).

$$V_3 = \frac{2.3(T_2)}{11600} (17.2 + 0.5 \text{ LOG}_{10} T_2 + 2 \text{ LOG}_{10} D_3) \quad (9)$$

$$V_4 = \frac{2.3(T_1)}{11600} (17.2 + 0.5 \text{ LOG}_{10} T_1 + 2 \text{ LOG}_{10} D_2) \quad (10)$$

where T_1 and T_2 are electrode temperatures ($^{\circ}\text{K}$), and D_2 and D_3 are the distance (meters). As stated above, the zero-current condition should be related to the applied diode voltage, since this is the parameter most easily obtained during an experiment. The relationship is obtained from Equations 9 and 10 and reference to Figure 2.

$$V_2 = V_4 - V_3$$

It is now possible to arrive at the voltage that must be applied to the diode in order to maintain zero-current conditions for a given set of electrode temperatures and diode spacing. However, the collector work function ϕ_C may be strongly influenced by the collector temperature and the effect of changes in ϕ_C should be examined.

Decreasing values of ϕ_C will do nothing to negate the model, only serving to raise the emission capability of the collector. Increasing values of ϕ_C are of great interest since at some point, the collector will become emission-limited and the model will change accordingly.

Referring to Figure 2, as ϕ_C increases, the value of V_3 will remain constant. However, when ϕ_C increases to the point that it is nearly equal to V_3 , the zero-potential-gradient plane will shift to the collector surface, reaching it when $\phi_C = V_3$. The potential energy diagram of Figure 3 applies to the situation for which $\phi_C \geq V_3$. At $\phi_C = V_3$, the distance $D_2 = D_1$ and the emitter temperature T_1 will establish a new emitter potential barrier V_7 in accordance with Equation 10. This new potential will be greater than the potential V_4 and will remain constant for

further increases in ϕ_c . Instead, further increases in ϕ_c will be reflected in a decrease in the required applied voltage V_2 . At $\phi_c = V_7$, the zero-current applied voltage is $V_2 = 0$. For values of ϕ_c greater than V_7 , the zero-current applied voltage V_2 must change polarity and act as a contributing potential for the emitter. The qualitative behavior of applied voltage as a function of increasing collector work function is shown in Figure 4. It is obvious that increases in ϕ_c can be tolerated to a certain point ($\phi_c < V_3$) but beyond that, variations in zero-current voltage and subsequent space-charge voltage-current parameters severely hinder the ability to correlate experimental voltage and current parameters with predicted diode behavior.

Results obtained from computer calculations based on the above zero-current model are shown in Figures 5 and 6. For the experimental phase of this study, the diodes used Philips Type B impregnated porous tungsten emitters with an operating temperature of $T_1 = 2100^\circ\text{F}$ (1422°K). Collector temperatures (T_2) between 1000 and 2100°F were considered along with diode mechanical spacings (D_1) between 0.004 and 0.010 inch.

In Figure 5, values for the potentials V_3 , V_4 and V_7 are presented as functions of collector temperature and diode mechanical spacing. In Figure 6, the applied voltage V_2 is plotted as $(V_4 - V_3)$ and $(V_7 - V_3)$ corresponding to the two conditions of collector work function; one ($\phi_c < V_3$) resulting in the virtual emitter being in the interelectrode gap and the

second ($\phi_c > V_3$) resulting in the virtual emitter being at the collector surface.

For the lower values of collector work function, as the collector temperature increases from 1000 to 2100°F, there is a marked increase in the collector potential barrier V_3 (about 1.7 to about 3 volts) until at 2100°F, the collector and emitter potential barriers (V_3 and V_4) are equal. At this point, the applied voltage necessary for zero-current conditions is $V_2 = 0$ and the diode experimental space-charge characteristic (V_2 plotted against diode current) will pass through the origin. This is the only condition for which this statement holds. Any other combination of collector work function and collector temperature will result in the necessity for a non-zero applied voltage to achieve zero-current conditions. Knowledge of collector temperature and work function is required before theoretical space-charge curves can be plotted, against which experimental data may be evaluated.

SPACE CHARGE MODEL (NON-ZERO CURRENT)

The non-zero current model is based on electron flow from the emitter being in excess of that from the collector. For this case, the applied diode voltage V_2 is used to raise the emitter Fermi level and the potential energy diagram is as shown in Figure 7. Again, the collector work function ϕ_c is first assumed to be less than the potential V_3 and the zero-potential-gradient plane is located in the inter-electrode gap. The resultant diode current is I_3 and the diode space-charge driving voltage is denoted by the potential V_1 . The distance D_4 is used to denote the position of a psuedo zero-potential-gradient plane referred to the collector and determined by the total diode current I_3 .

The main aim of this study was to develop a set of theoretical data based on this model and from which a set of master space-charge curves (applied diode voltage vs. diode current) could be plotted for various collector temperatures. Tests run on an operating diode would then be compared with the master curves. The computer program developed to calculate these theoretical data used the following procedure.

1. A mechanical spacing D_1 was established.
2. A spacing D_2 , the distance from the emitter surface to the virtual emitter plane, was assumed. This also resulted in a value for $D_3 = D_1 - D_2$.

3. The emitter and collector currents (I1 and I2) were calculated from Equations 4 and 5.
4. The diode current $I3 = I1 - I2$ was calculated subject to the condition $I3 > 0$. If this condition was not met, the allowable range of D2 had been exceeded.
5. A collector space-charge condition was assumed ($\phi_c < V3$) and the distance D4 was determined from the diode current I3 using a transposed form of Equation 5.

$$D4 = \left(\frac{7.729 \times 10^{-12} (T2)^{3/2} A}{I3} \right)^{1/2}$$

6. The space-charge driving voltage V1 was determined using a transposed form of Child's formulation (Equation 1) for space-charge current.

$$V1 = \frac{(D5)^{4/3} (I3)^{2/3}}{(2.34 \times 10^{-6} A)^{2/3}}$$

$$\text{with } D5 = D1 - D2 - D4$$

7. The potentials V3 and V4 were calculated using Equations 9 and 10.
8. The voltage that must be applied to diode to maintain the specific current condition was calculated.

$$V2 = V1 + V3 - V4$$

As with the zero-current analysis, the effect of increasing ϕ_c is of great interest. The model is valid subject to the condition $\phi_c < V3$. For a given diode current level, the potential V4 will remain fixed regardless of increases in ϕ_c beyond

$\phi_C = V_3$, and these increases in ϕ_C will be matched directly by required increases in the diode applied voltage V_2 .

When space-charge data (V_2 vs. I_3 for specific values of D_1 , T_1 , and T_2) are calculated from this model, a set of master curves may be plotted; as shown on Figures 8 through 21. As long as $\phi_C < V_3$, tests run on an operating diode should agree with the master curves. If ϕ_C increases beyond V_3 , the experimental curve will depart from the master curve and indicate higher applied voltage for a given current level. The deviation will be equal to the increase in ϕ_C beyond its critical value of V_3 .

EXPERIMENTAL PROGRAM

The final computer program used to work out the parameters of the zero and non-zero-current space charge models was based on an emitter temperature of 2100°F, a collector temperature range of 1000-2000°F and a diode spacing range of 0.001 - 0.010 inch. Results of the zero-current analysis are presented in Figures 5 and 6; master curves for non-zero current conditions are shown on Figures 8 through 21 along with test results from two temperature excursion runs (1600, 1400, 1200, 1000, 1200, 1400, 1600°F) performed as part of a pressure transducer program conducted for NASA under contract NAS3-4170 (Reference 2).

The test unit was the final design configuration of a pressure transducer using a thermionic diode sensor to transform the mechanical motion of a refractory alloy pressure capsule into a suitable electrical output. The thermionic diode sensor included two diodes; one whose spacing decreased with pressure applied to the transducer and another whose spacing was fixed. The currents corresponding to these diodes were called the active current (I_a) and reference current (I_r), respectively.

Testing was performed in a high-vacuum environment (10^{-8} torr) with controllable ambient (collector) temperature. The transducer signal conditioning system was designed with a capability of maintaining a 2100°F emitter temperature regardless of ambient temperature and monitoring the space charge parameters of each diode. Current and voltage signals were delivered to an X-Y recorder. A potentiometer voltage control was used for continuous adjustment of the diode voltage, resulting in the gen-

eration of a continuous space charge curve by the recorder.

In Figures 8 through 21, the computer-calculated master curves are shown solid while the experimental runs are shown dotted. One curve is shown for the reference current I_r , which does not change with pressure. Three curves are shown for the active current I_a ; corresponding to pressures of 0, 40 and 80 psia applied to the transducer.

Generally, the experimental space charge curves supported the model and agreed quite well with the master curves for low applied-voltage levels (up to about 3 volts). Moreover, there was an obvious negative voltage requirement for zero-current. Both of these facts indicated that the collector work function was indeed low and probably was close to the critical values above which the models are no longer valid. As the diode current increases, there will be a tendency for the collector surface to clean due to electron bombardment. The work function of a clean surface of the refractory alloy used for the collectors is about 5 volts. Considering the V3 curves of Figure 5, it was apparent that the zero and low-current values of collector work function were well below 2.5 volts. In this context, the deviation, at high-current levels, of the experimental data from the master curves was surely a direct result of increases in the collector work function. In addition, the combination of changing current levels and collector temperature could introduce non-repeatable work function effects.

To obtain a meaningful evaluation of the diode, it was obvious that diode operation must be limited to regions where (1) the collector work function is constant or (2) changes in the collector work functions are repeatable and may be compensated.

SUMMARY OF RESULTS

Under ordinary circumstances, the analysis of the operation of a vacuum thermionic diode in the space charge limited regime is justified in neglecting collector contributions. These contributions include both emission effects, which contribute to the diode current, and surface effects, which may cause undesired changes in collector work function.

A refined space-charge model has been developed which includes emission from both the emitter and collector electrodes, an understanding of the effect of increasing collector temperature, and allows for an evaluation of any variations in collector work function.

Computer calculations have allowed the construction of a set of master space charge curves against which the experimental diode may be compared. Since the applied diode voltage is the most readily available test parameter, the master curves have been established from calculations resulting in diode current and applied voltage parameters.

Space charge runs made on experimental diodes over a collector temperature of 1000-1600°F resulted in general agreement with the master curves. This agreement was most evident at low voltage/current values. As the diode current increased, the experimental data deviated from the master curves. The deviations were considered to be a direct result of increases in collector work function.

It appeared that the model developed was capable of being used as an evaluation technique for vacuum thermionic diodes operating in an environment which results in collector temperatures exceeding 1000°F. Moreover, comparison of the experimental data with the calculated master curves could be used to determine the optimum operating voltage/current values. Ideally, the diode should be operated such that the collector work function is constant or changes in the collector work function are repeatable and may be compensated. If these conditions are not met, diode operation will be non-repeatable.

REFERENCES

1. W. B. Nottingham; "The Thermionic Diode as a Heat-to-Electrical-Power Transducer", Direct Conversion of Heat to Electricity, e. by J. Kaye and J. A. Welsh, M.I.T. Summer Session, July 1959, Chapter 2.
2. A. J. Cassano; Topical Report, Pressure Measuring Systems for Closed Cycle Liquid Metal Facilities, NASA CR- To be published.

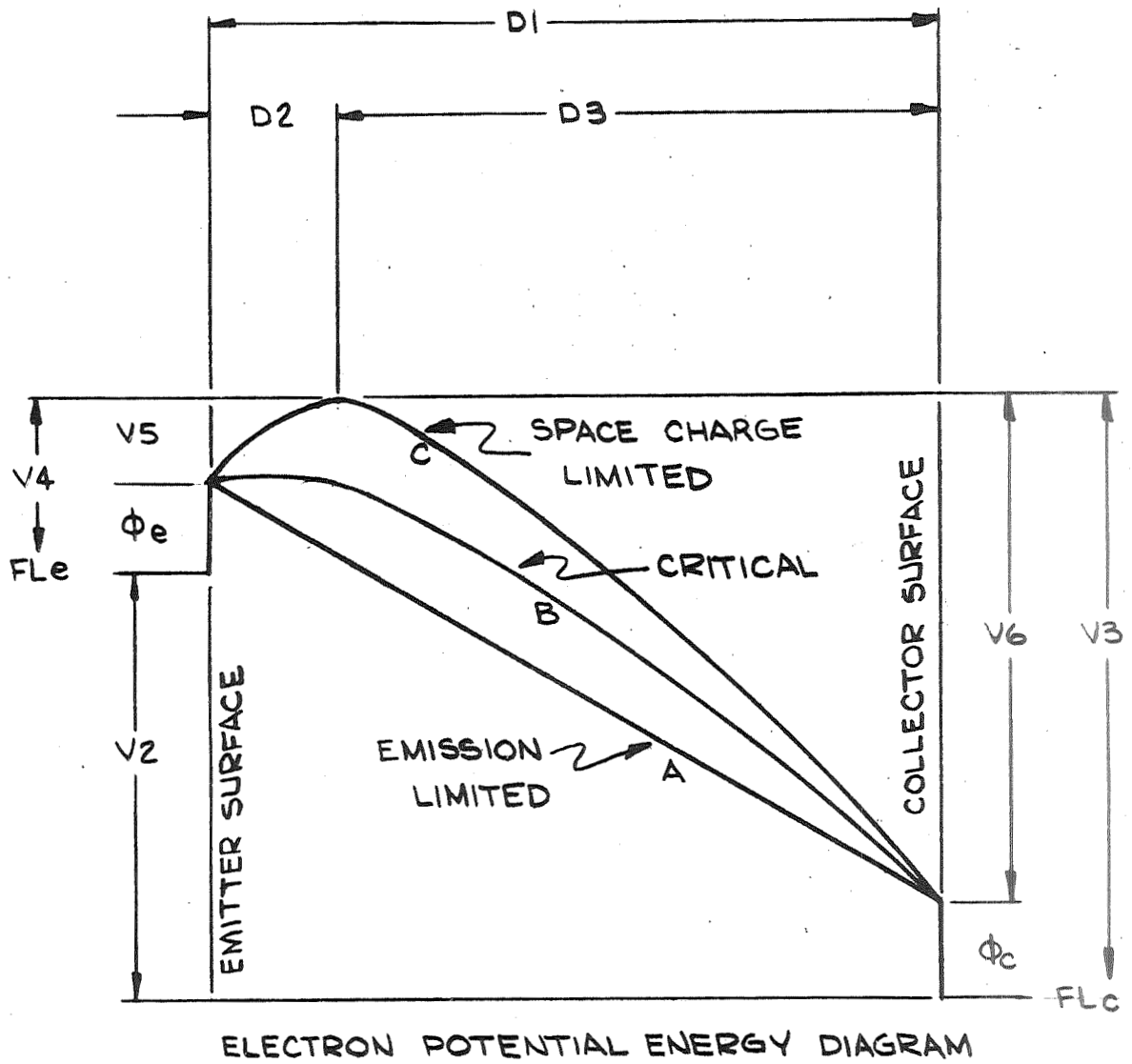
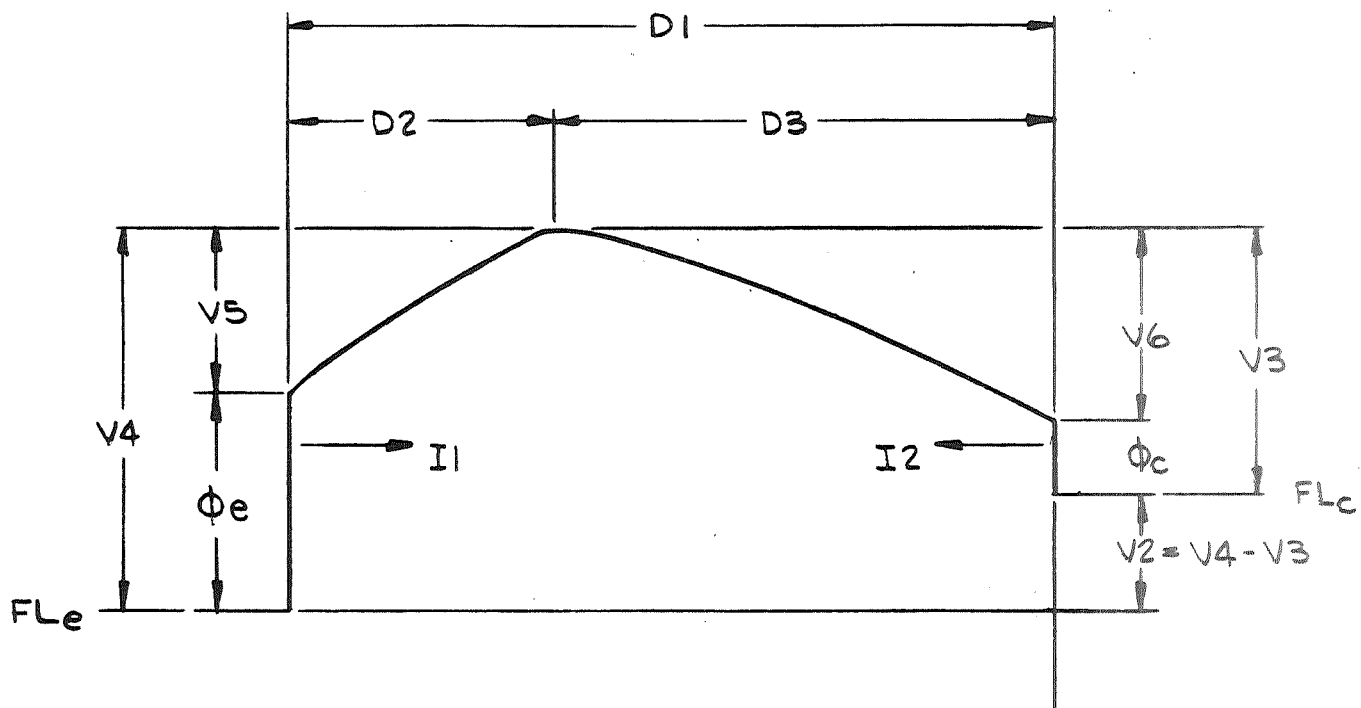
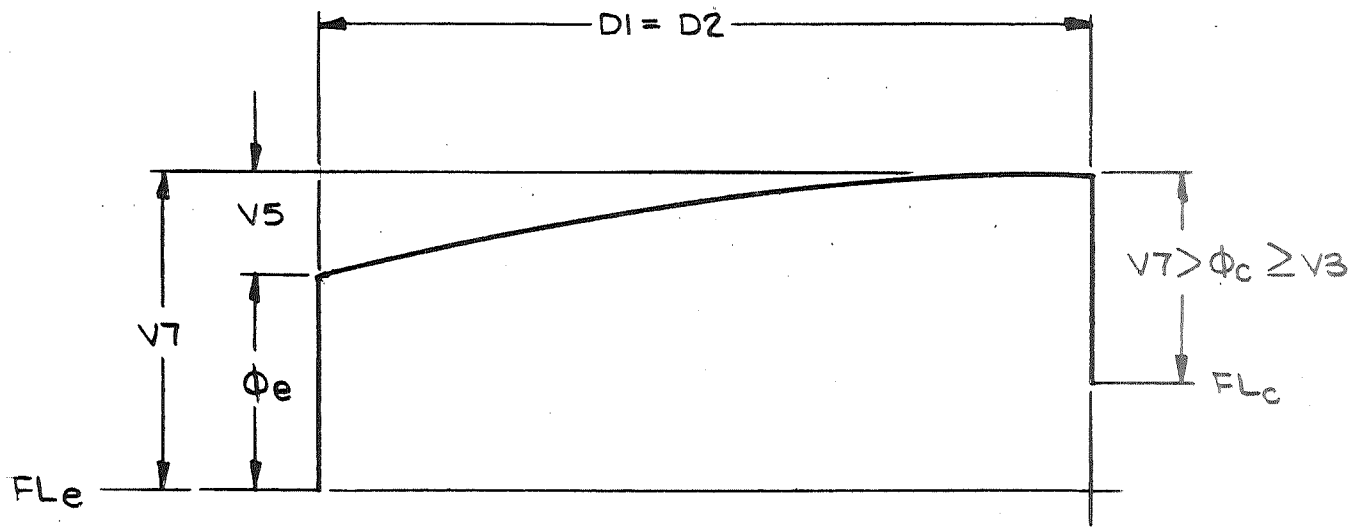


FIGURE 1



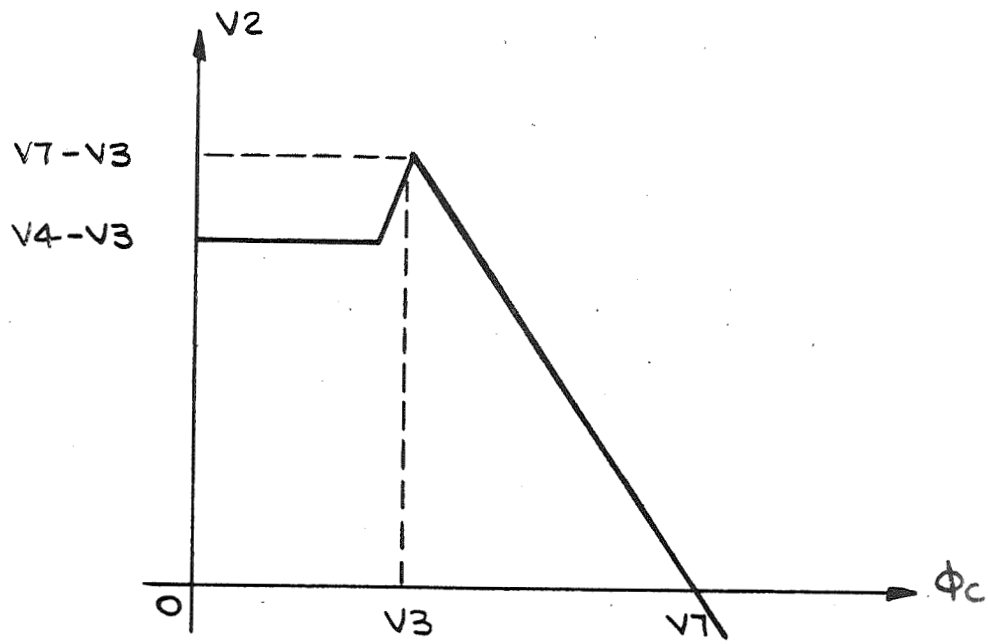
ZERO-CURRENT POTENTIAL ENERGY DIAGRAM
LOW COLLECTOR WORK FUNCTION

FIGURE 2



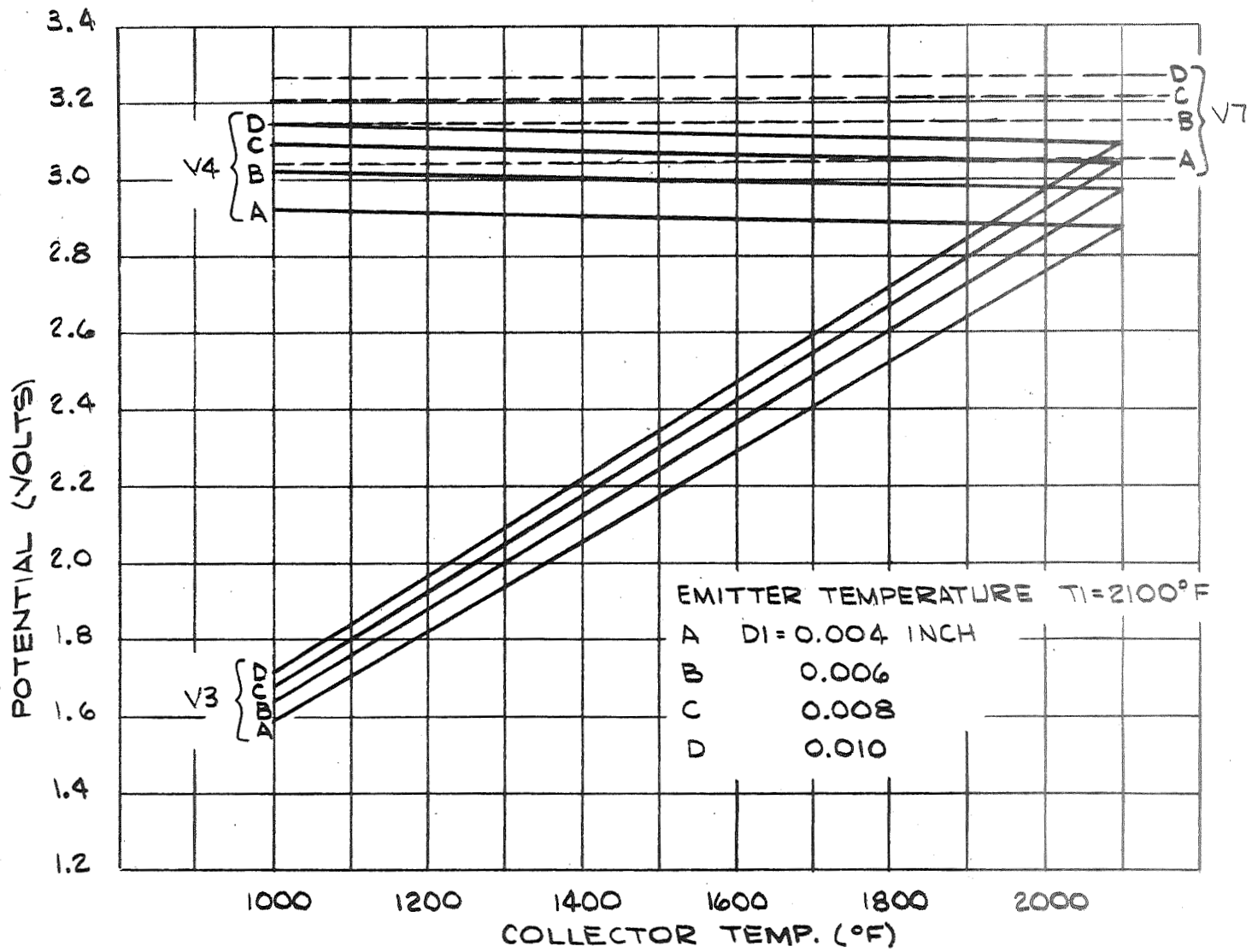
ZERO-CURRENT POTENTIAL ENERGY DIAGRAM
HIGH COLLECTOR WORK FUNCTION

FIGURE 3



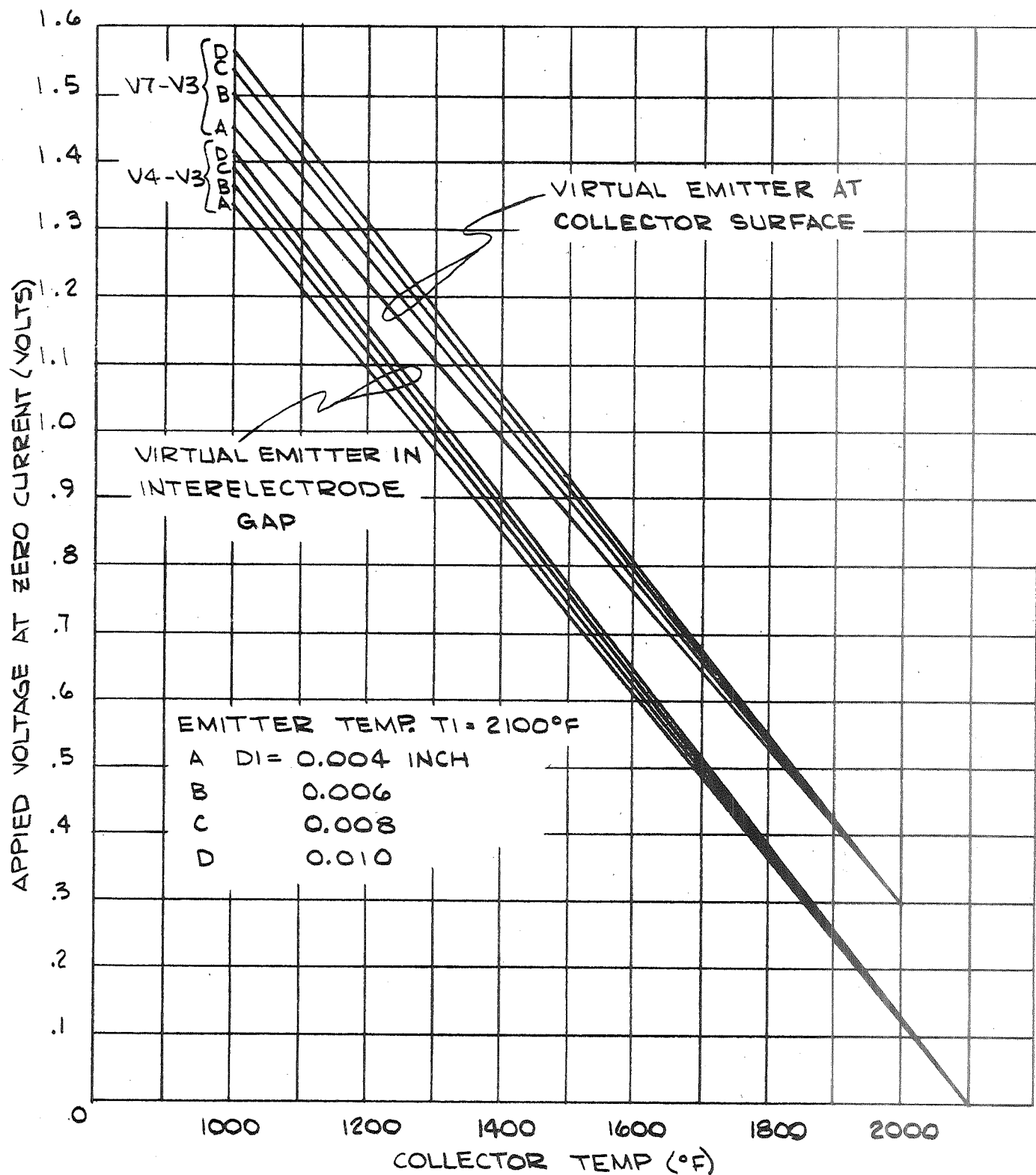
APPLIED DIODE VOLTAGE AS FUNCTION OF COLLECTOR WORK FUNCTION

FIGURE 4



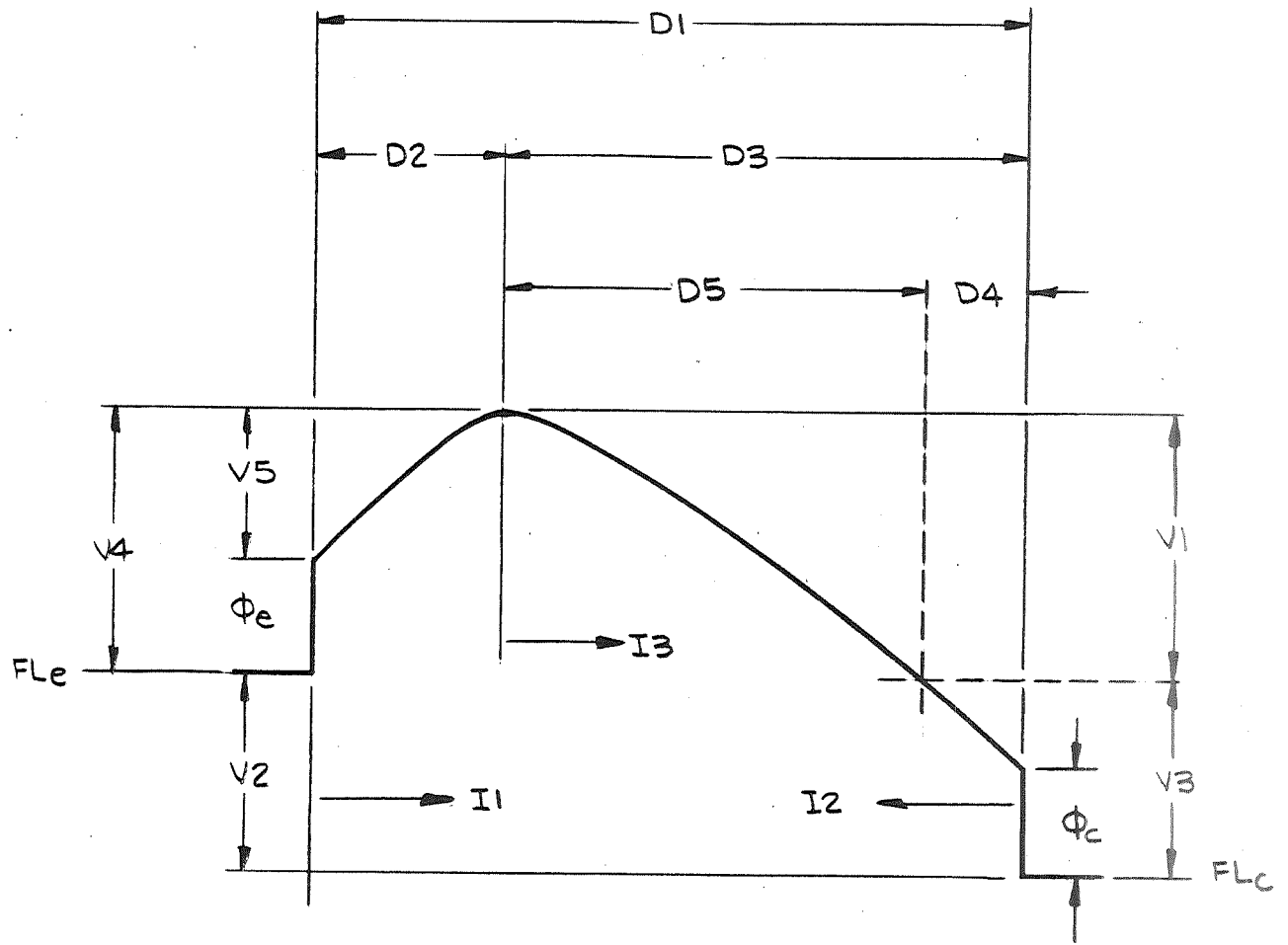
ZERO-CURRENT POTENTIALS AS FUNCTION OF COLLECTOR TEMPERATURE

FIGURE 5



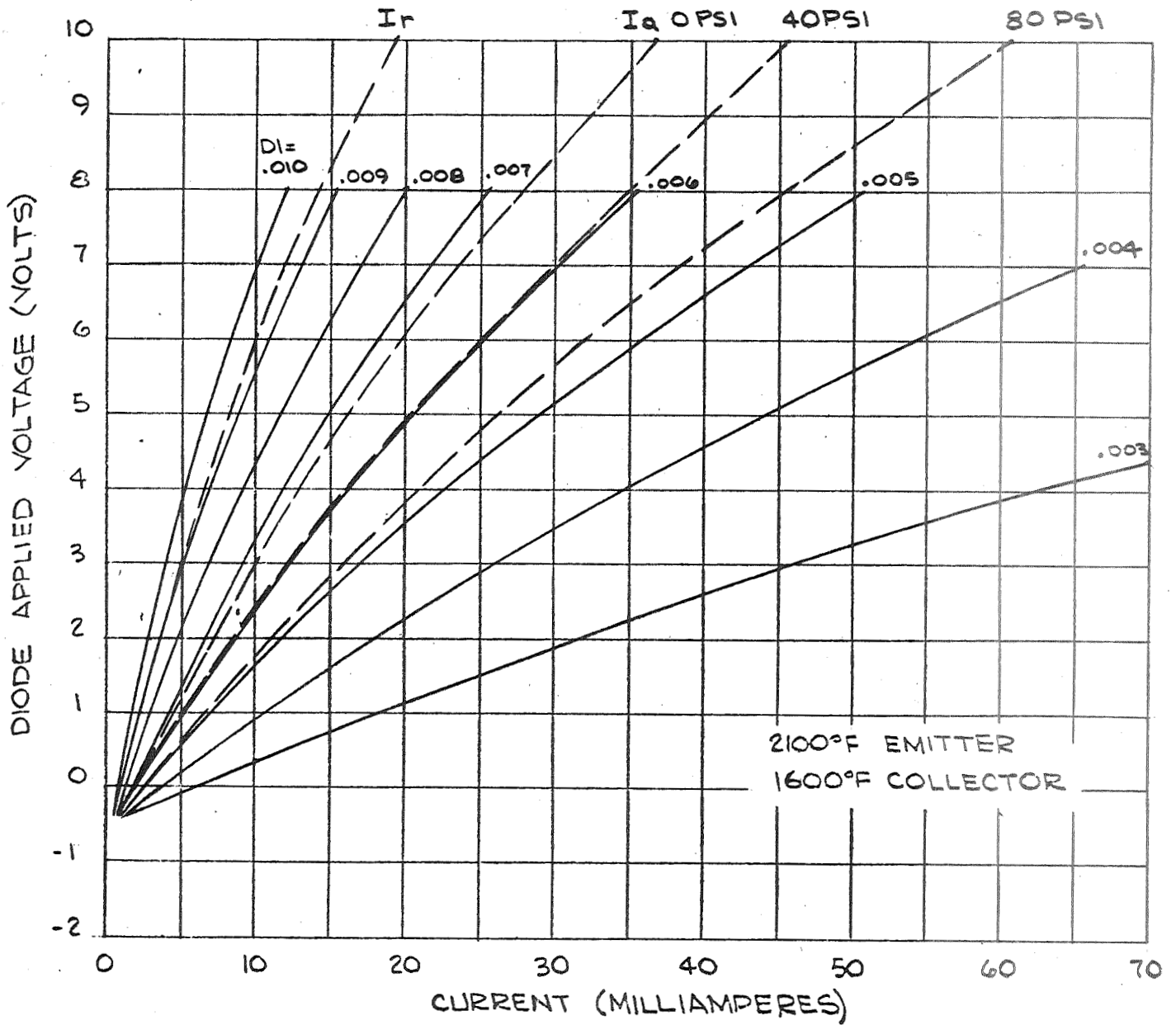
APPLIED DIODE VOLTAGE AS FUNCTION OF COLLECTOR TEMPERATURE

FIGURE 6



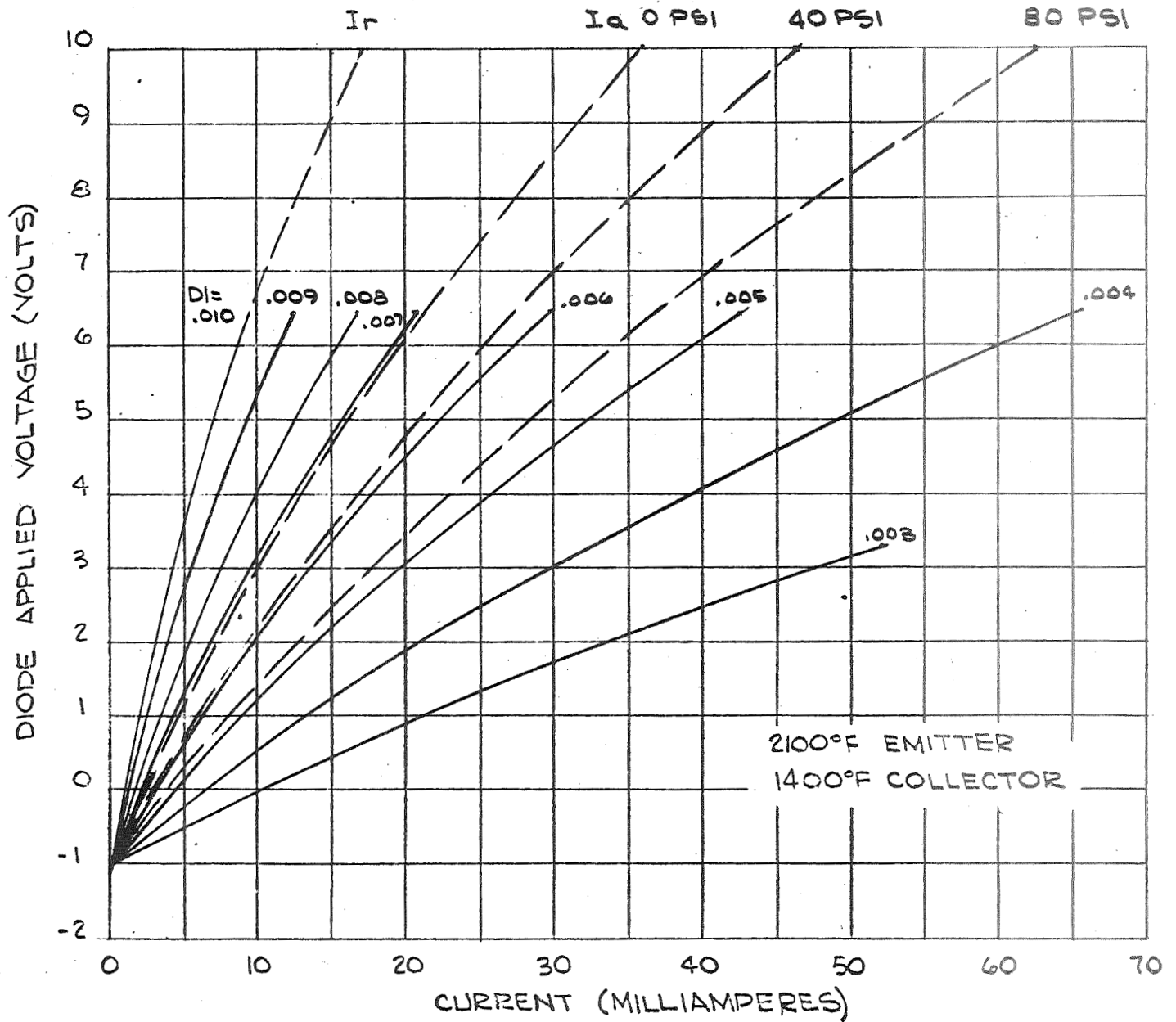
NON-ZERO-CURRENT POTENTIAL ENERGY DIAGRAM

FIGURE 7



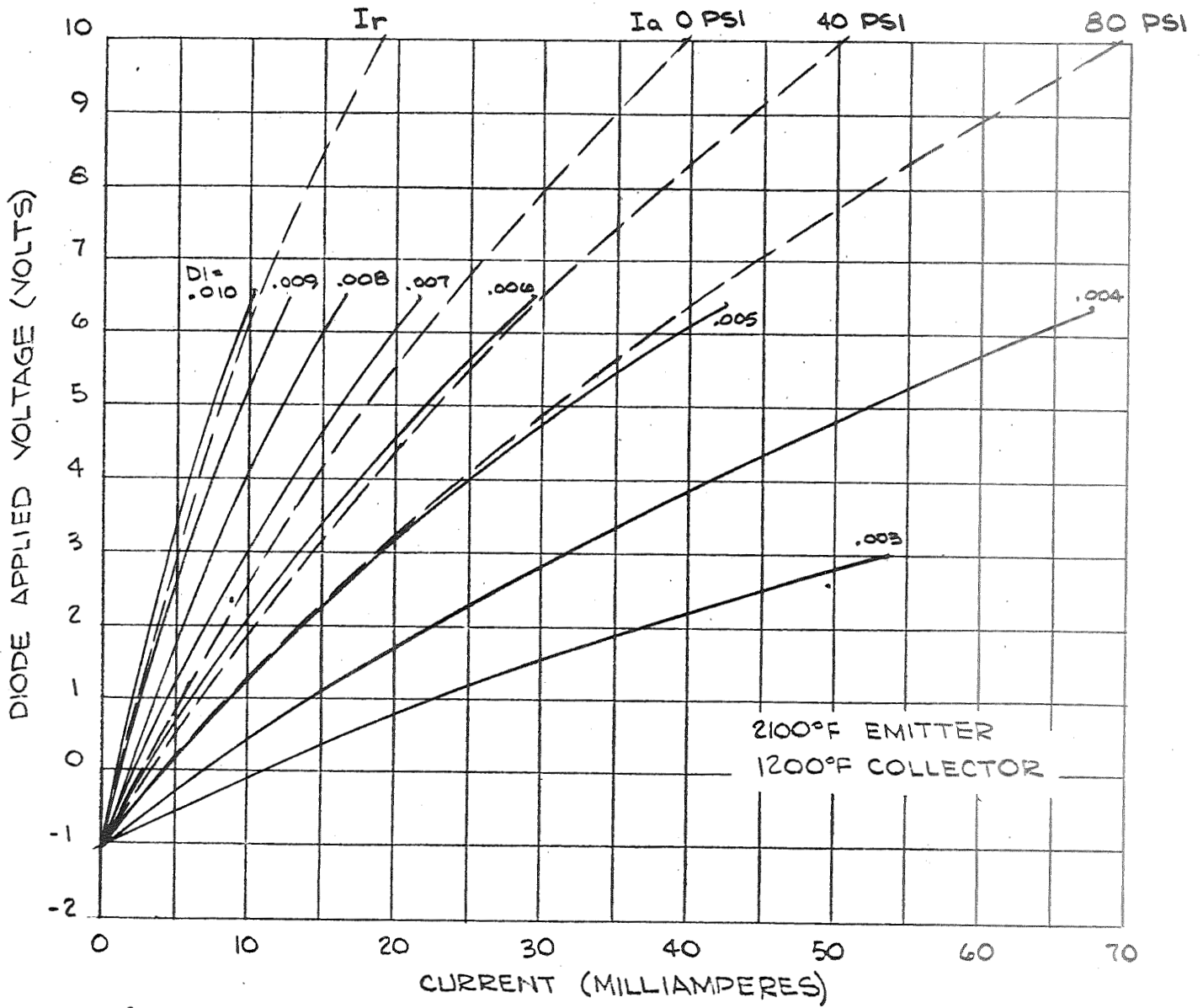
SPACE CHARGE CURVES 1600°F COLLECTOR

FIGURE 8



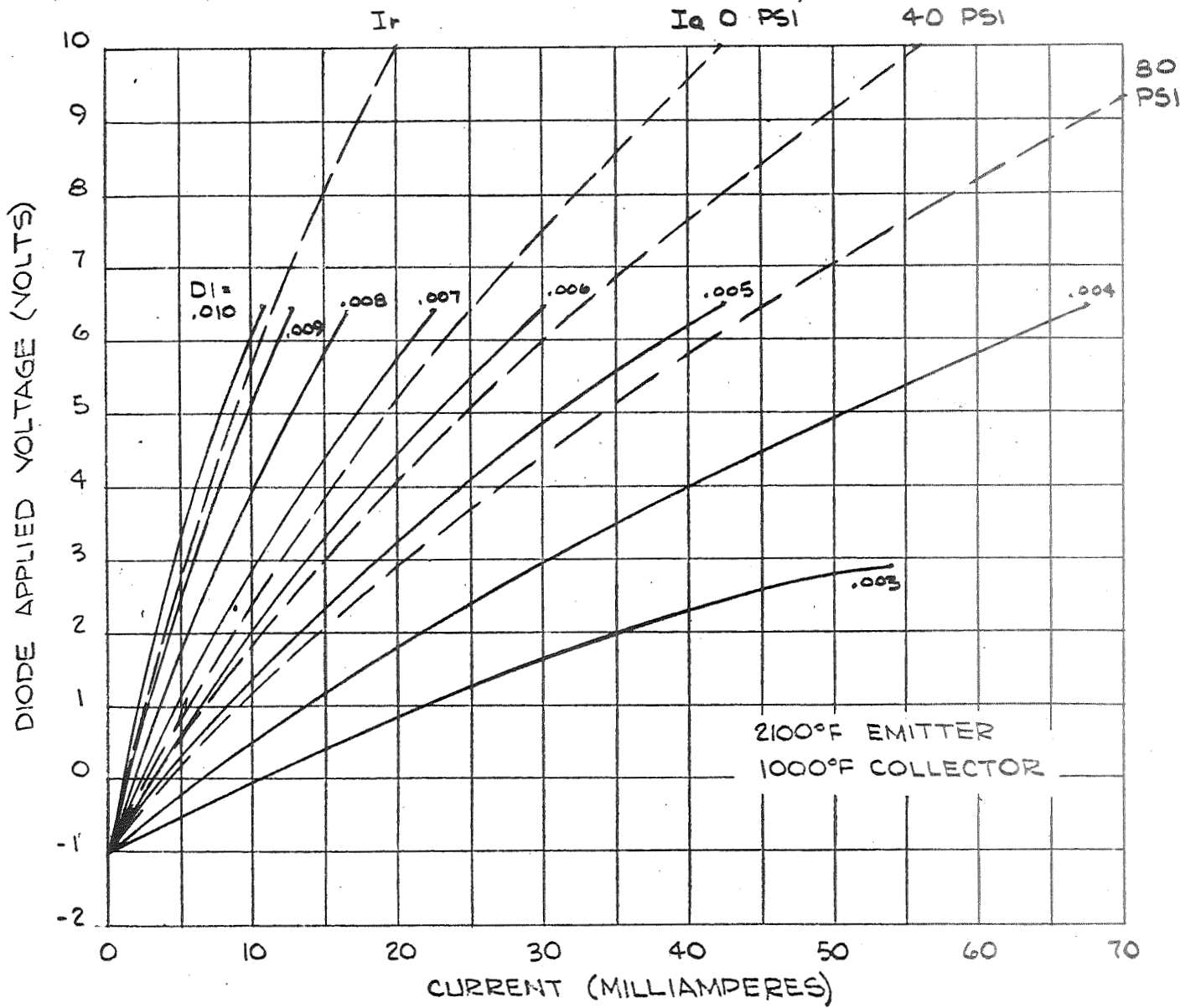
SPACE CHARGE CURVES 1400°F COLLECTOR

FIGURE 9



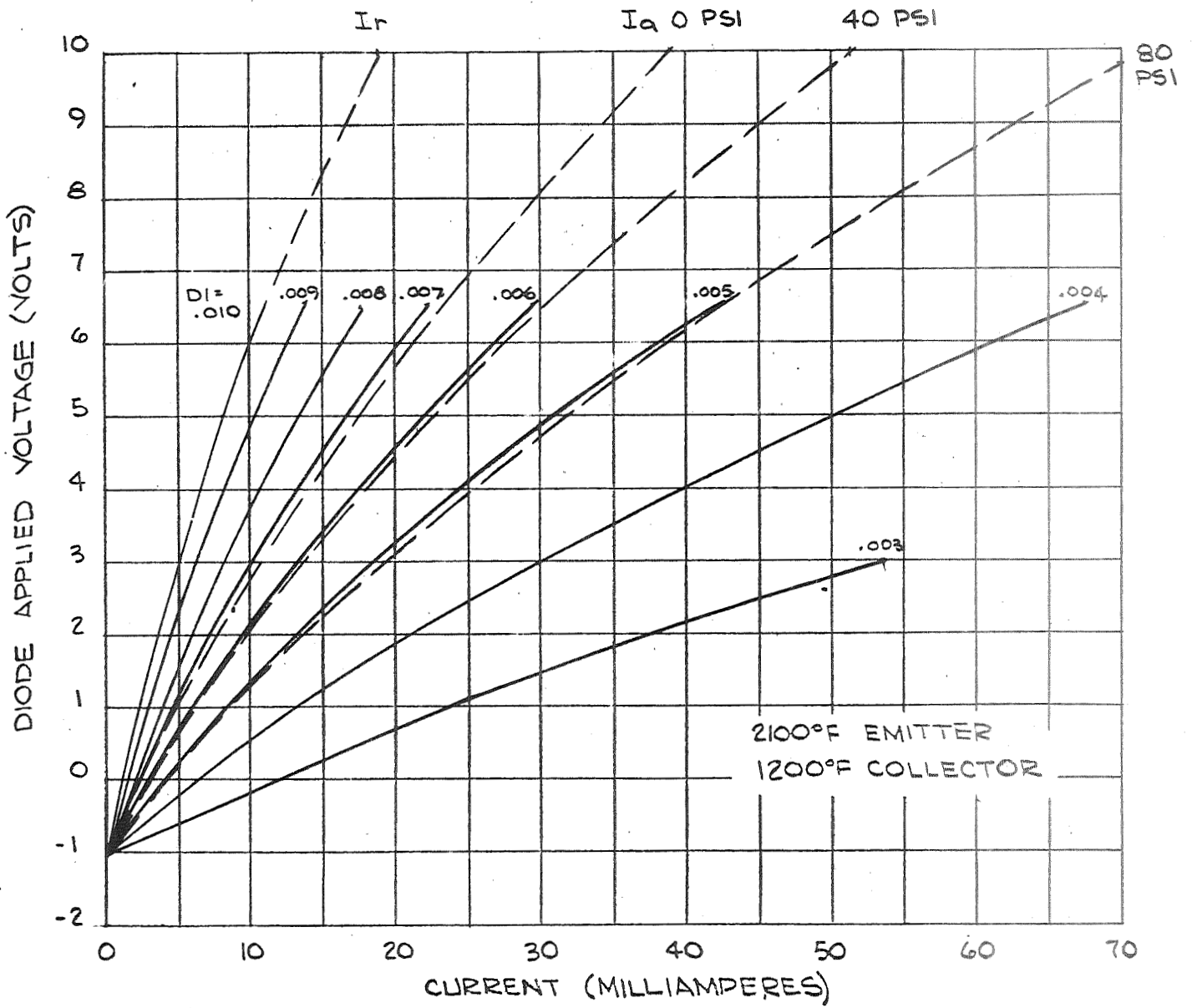
SPACE CHARGE CURVES 1200°F COLLECTOR

FIGURE 10



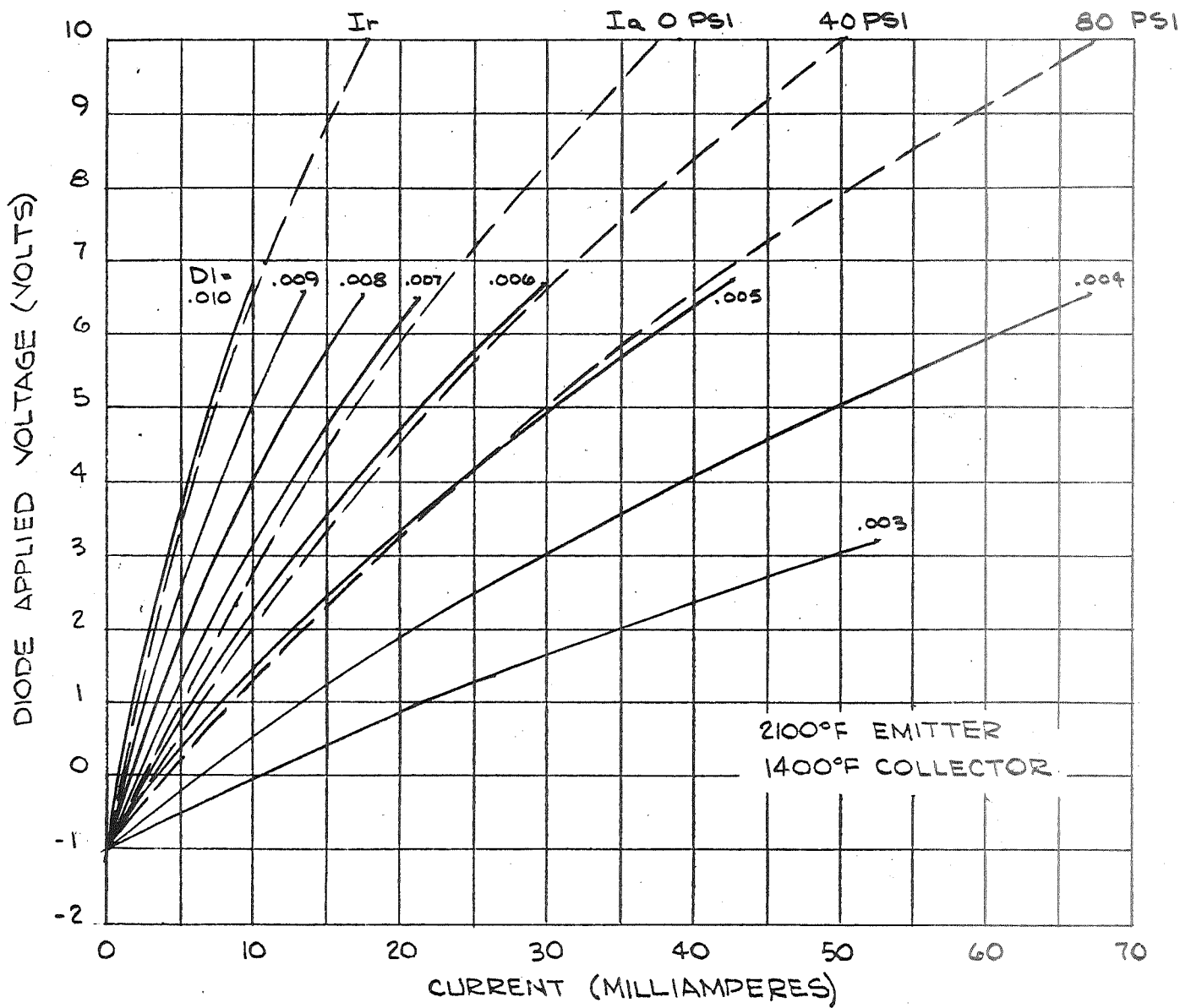
SPACE CHARGE CURVES 1000°F COLLECTOR

FIGURE II



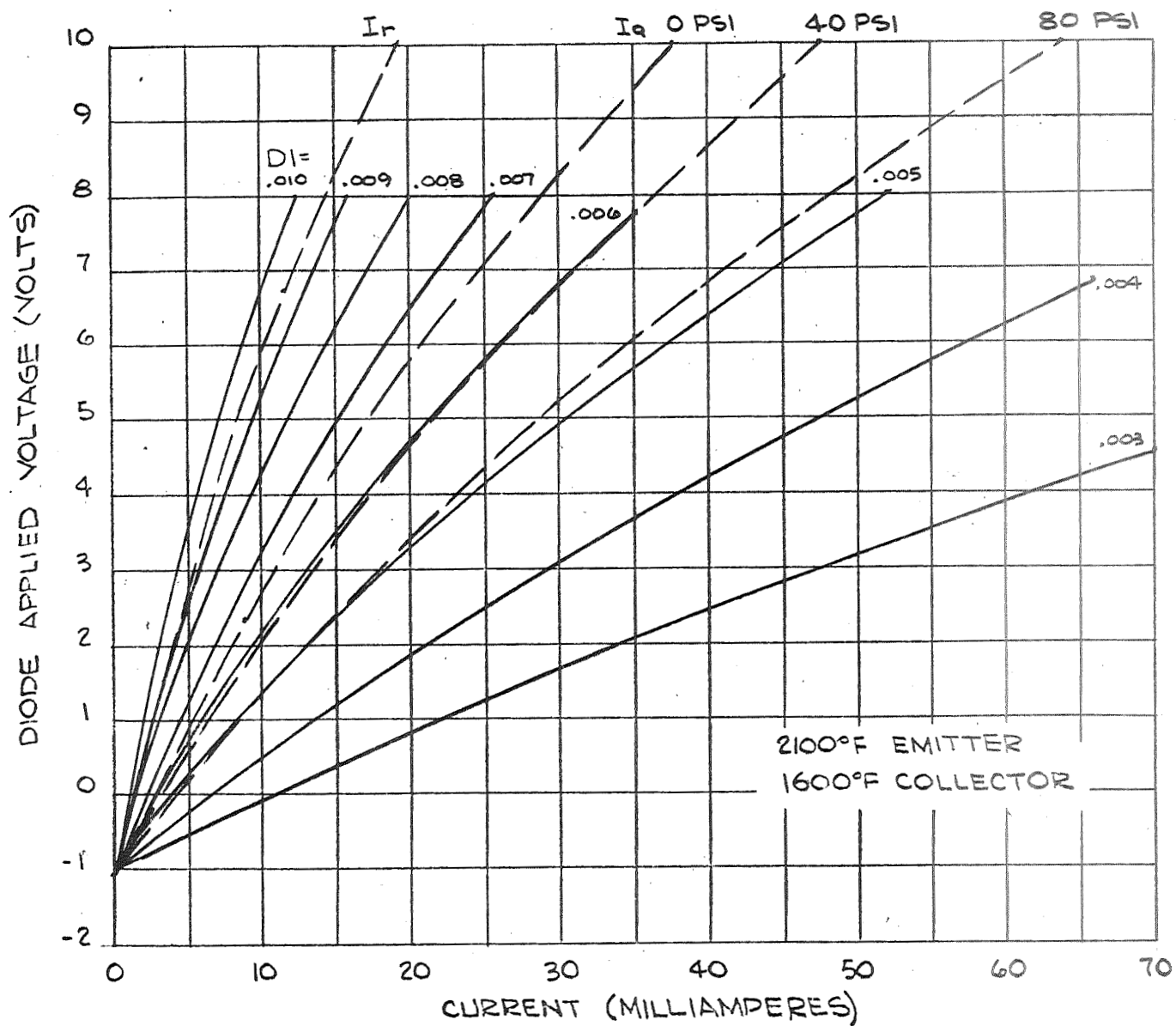
SPACE CHARGE CURVES 1200°F COLLECTOR

FIGURE 12



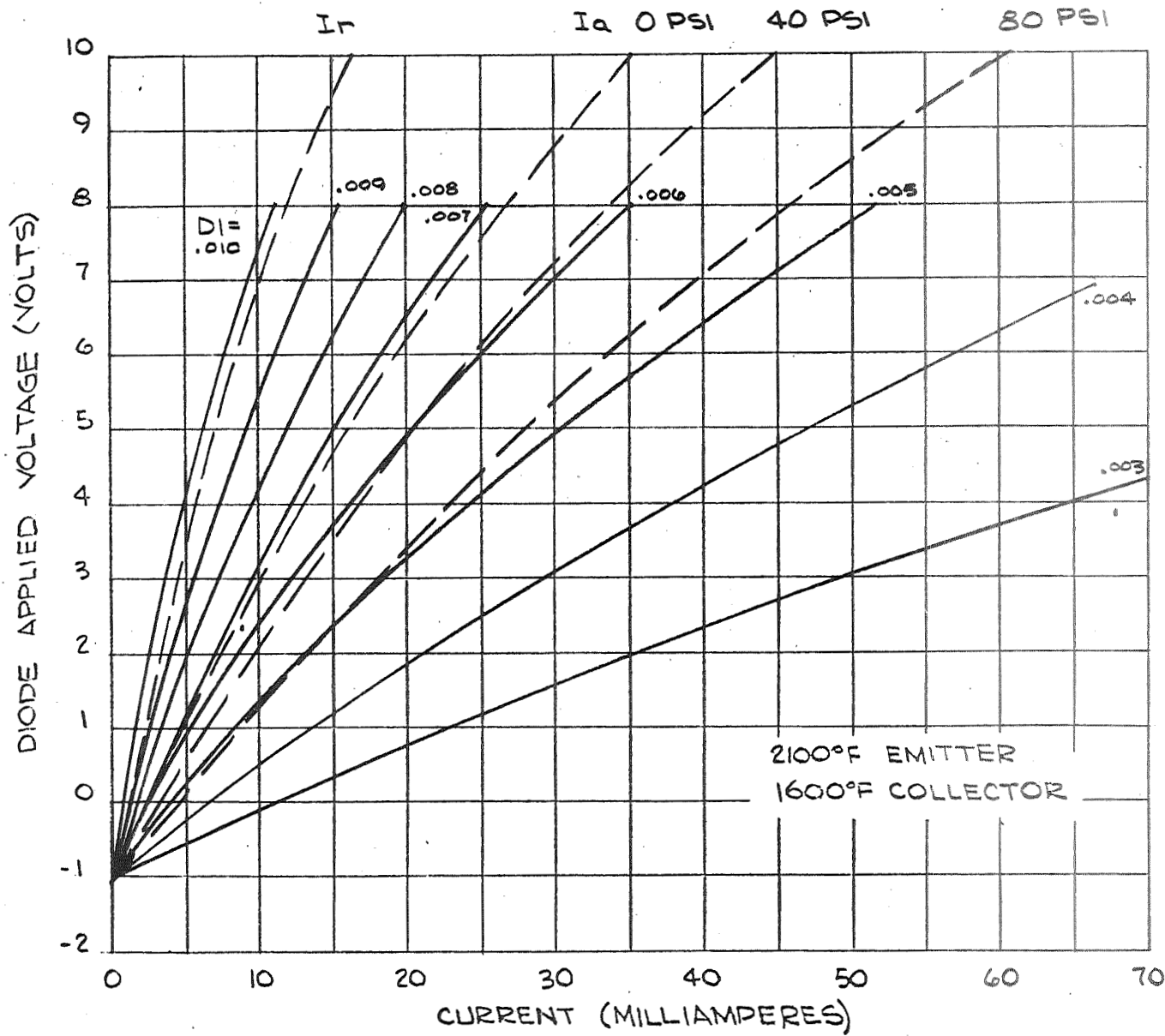
SPACE CHARGE CURVES 1400°F COLLECTOR

FIGURE 13



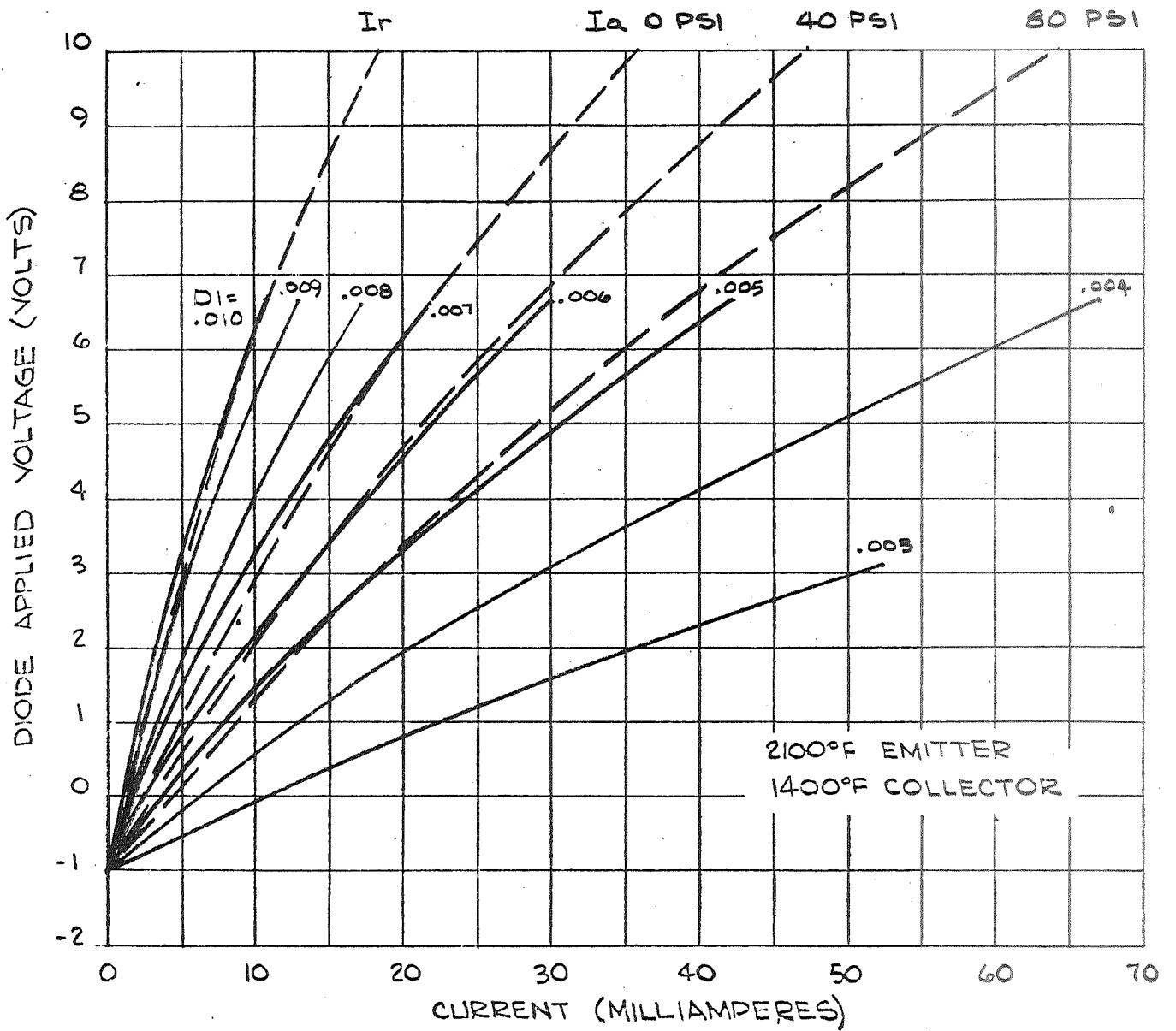
SPACE CHARGE CURVES 1600°F COLLECTOR

FIGURE 14



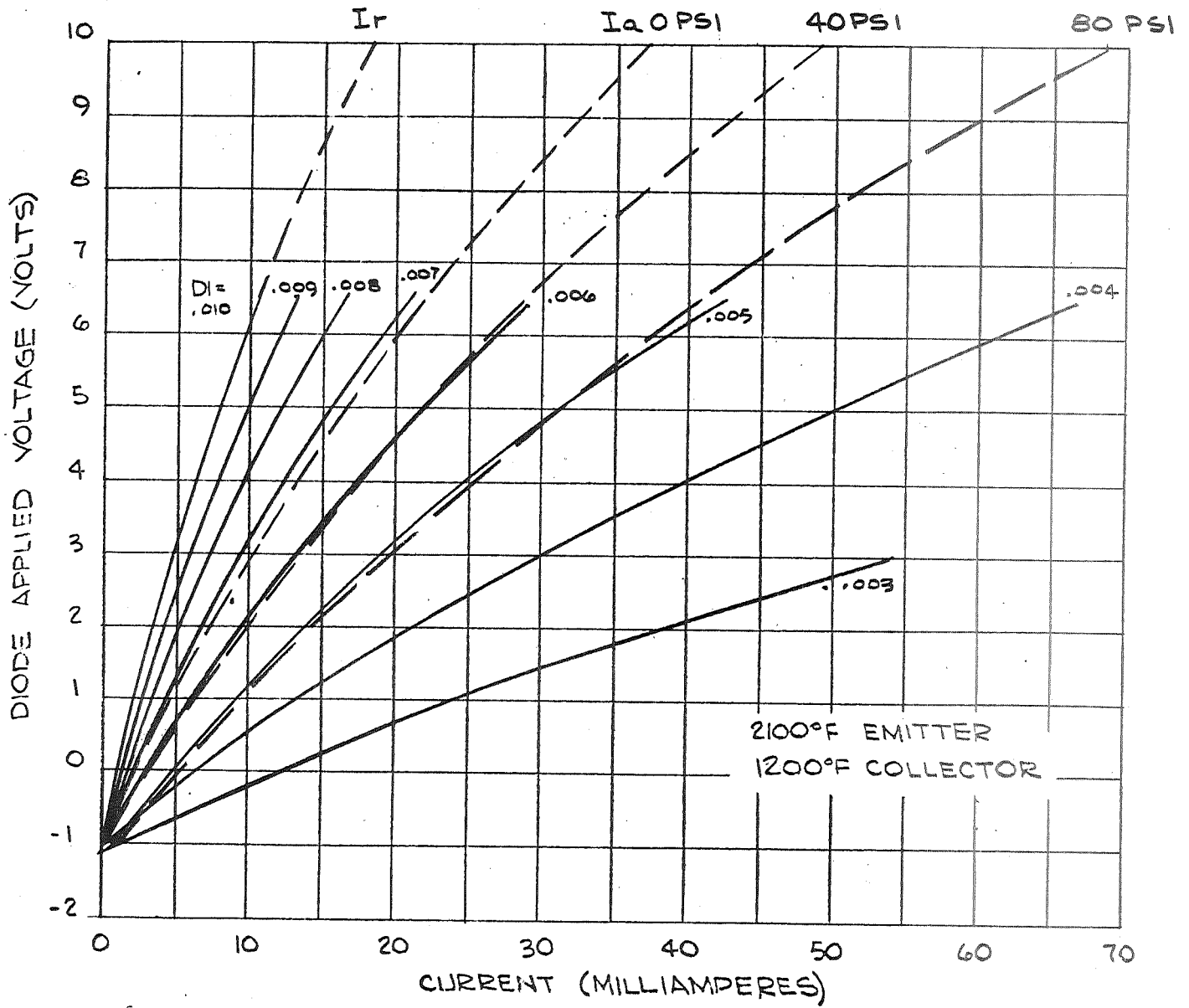
SPACE CHARGE CURVES 1600°F COLLECTOR

FIGURE 15



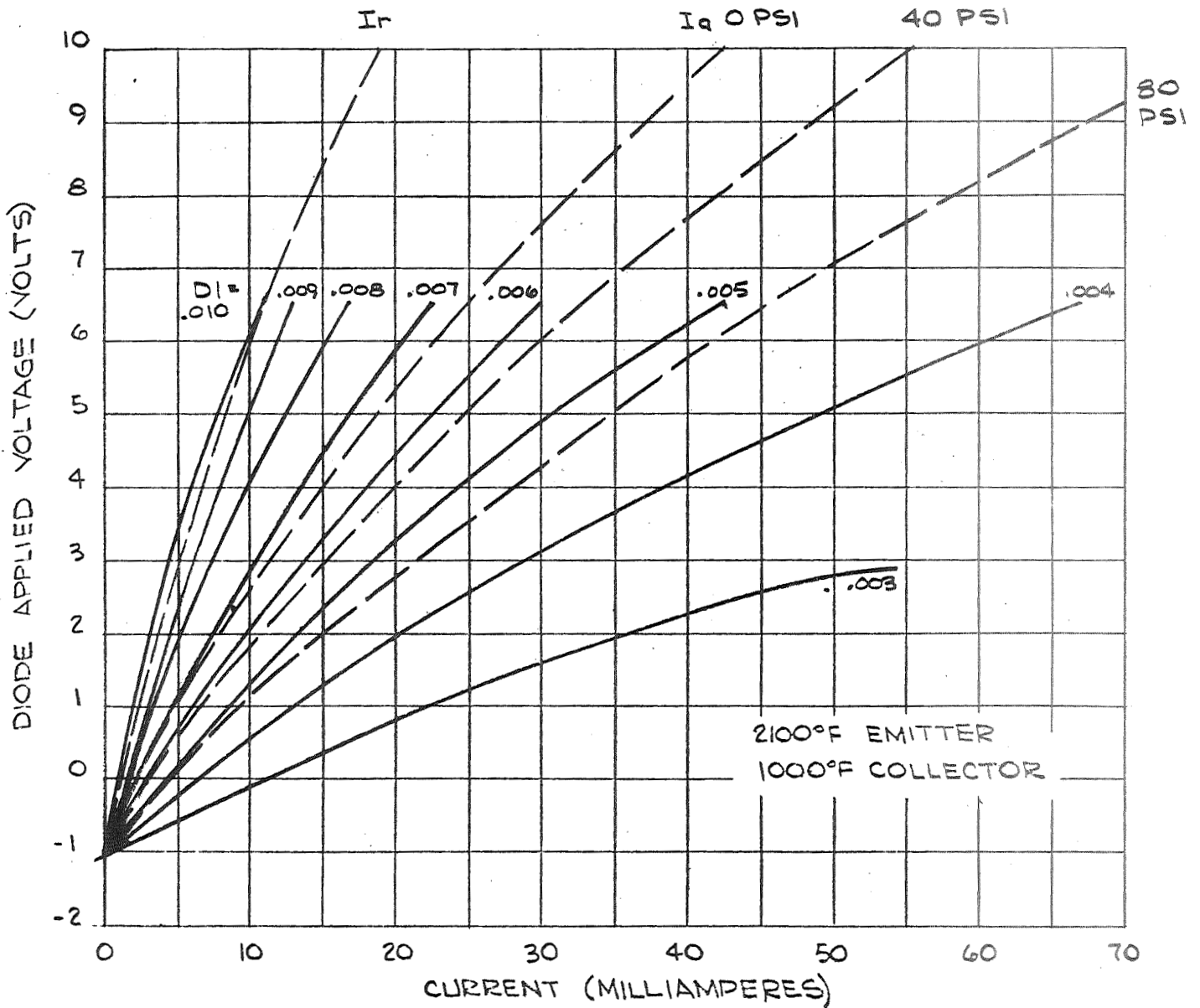
SPACE CHARGE CURVES 1400°F COLLECTOR

FIGURE 16



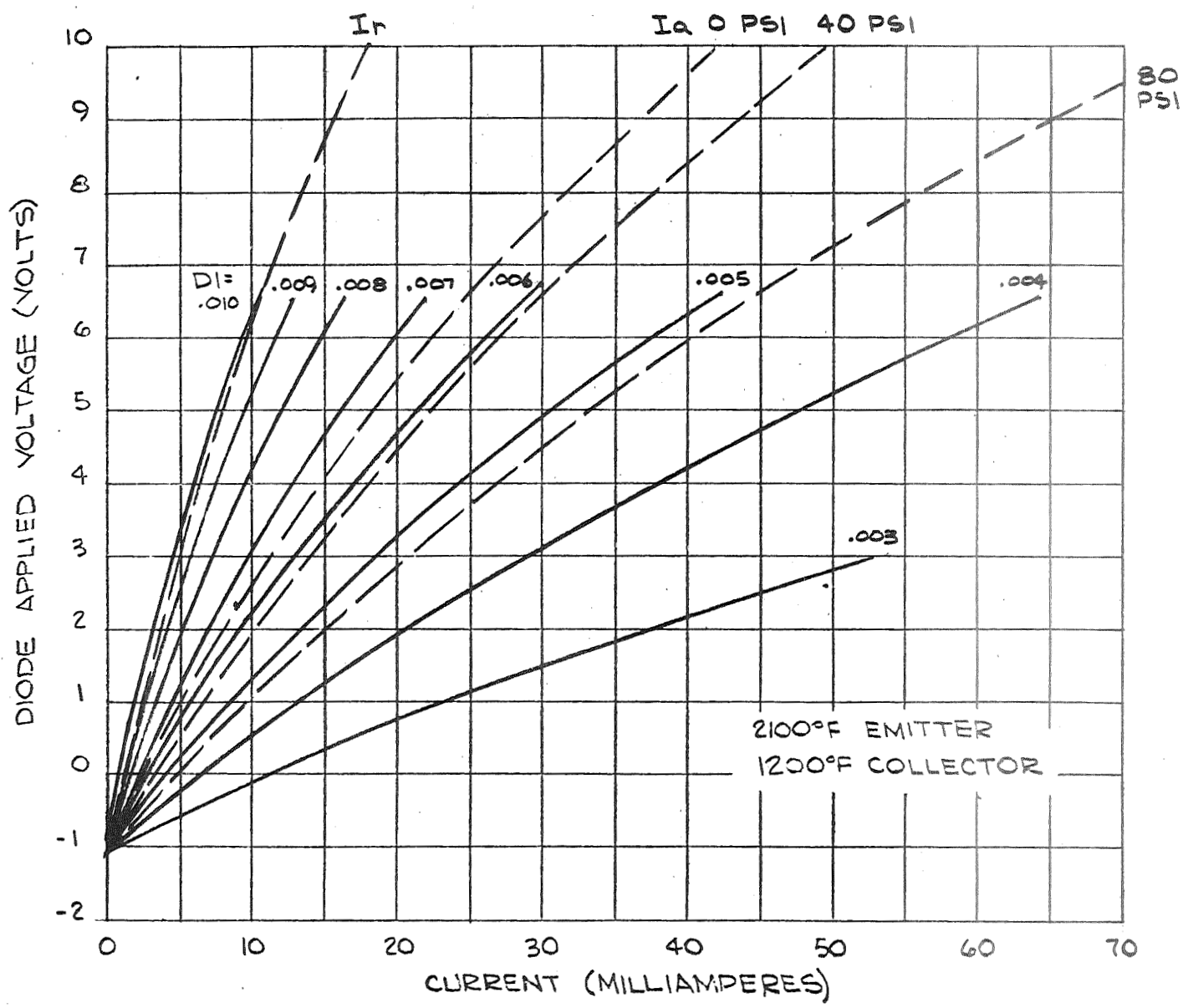
SPACE CHARGE CURVES 1200°F COLLECTOR

FIGURE 17



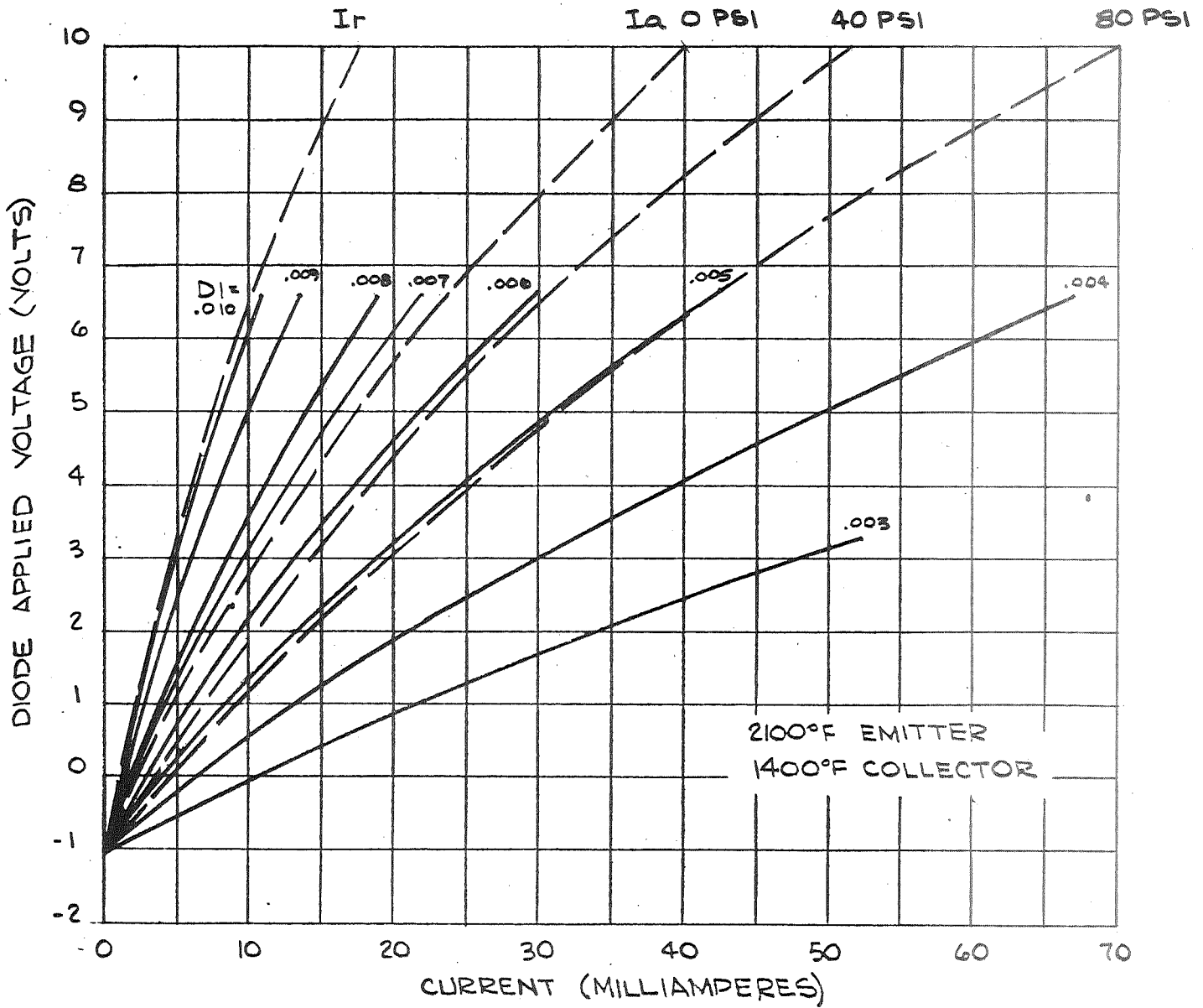
SPACE CHARGE CURVES 1000°F COLLECTOR

FIGURE 18



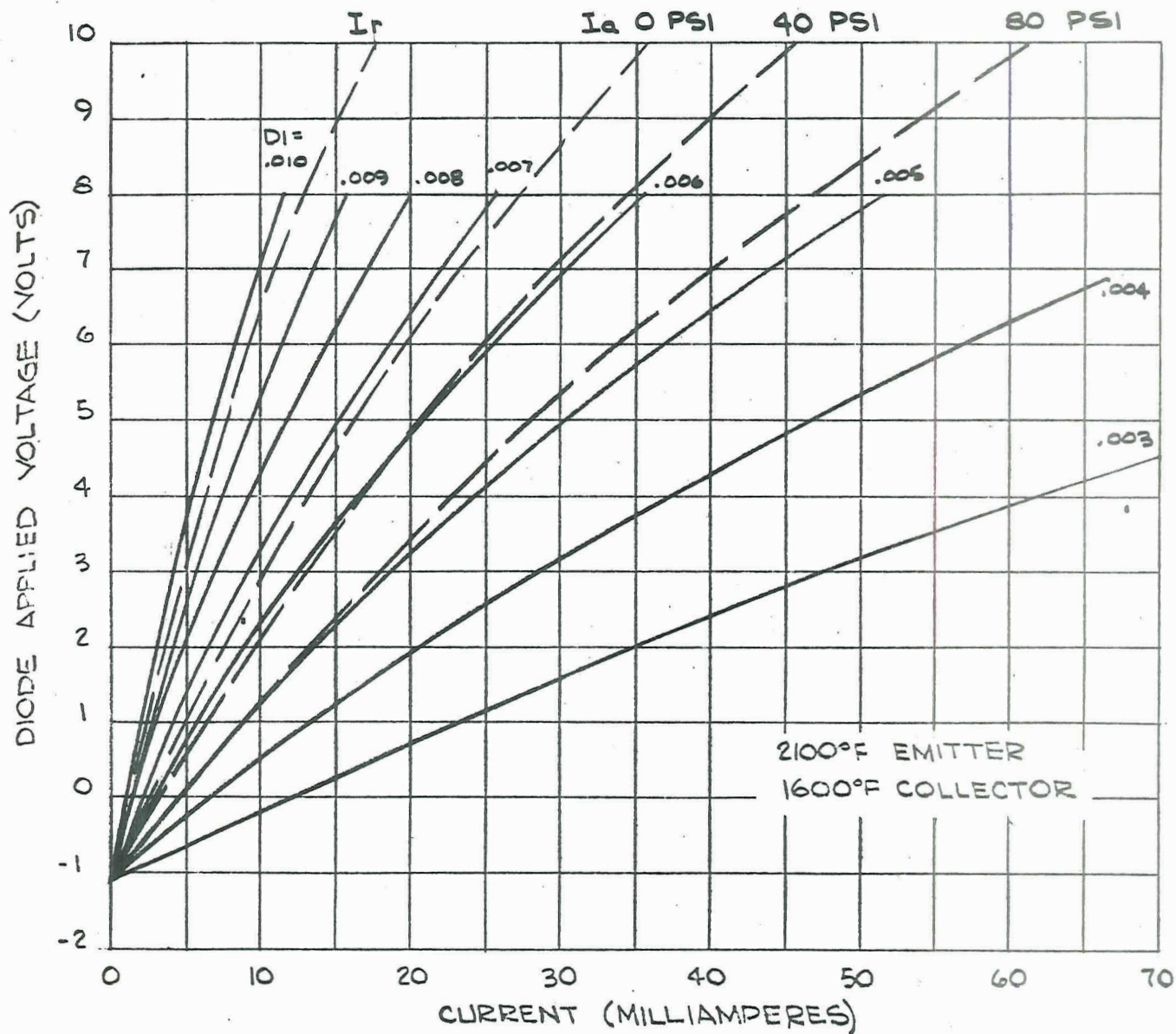
SPACE CHARGE CURVES 1200°F COLLECTOR

FIGURE 19



SPACE CHARGE CURVES 1400°F COLLECTOR

FIGURE 20



SPACE CHARGE CURVES 1600°F COLLECTOR

FIGURE 21